PISCES: A Spectral Element Code to Tackle Minor Mixing Processes for Astrophysical and Oceanographic Applications

Justin Brown
Pascale Garaud
Nic Brummell
Gary Glatzmaier

October 2, 2015

Double-diffusive convection defines instabilities in nominally stable fluids with two opposing buoyant fields.

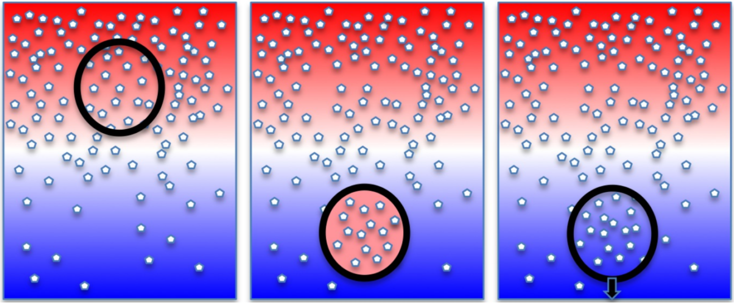
[1]

Figure: Fingering (FC; also Thermohaline, Thermocompositional) Convection

[1](Garaud, 2014)

Double-diffusive convection defines instabilities in nominally stable fluids with two opposing buoyant fields.

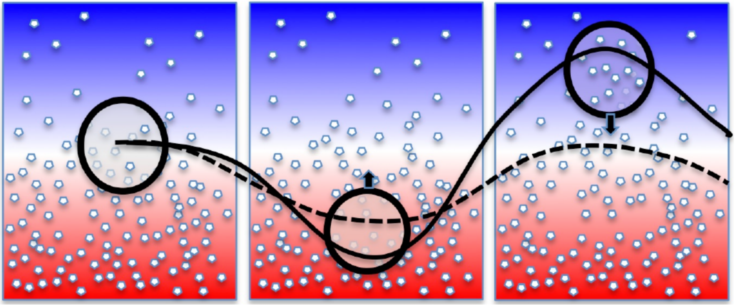 [1]

Figure: Oscillatory Double-Diffusive Convection (ODDC; also sometimes Semi-Convection)

[1](Garaud, 2014)

Massive stars ($> 8M_\odot$) are significant because they produce a large fraction of the heavy elements either during their evolution or in supernovae.

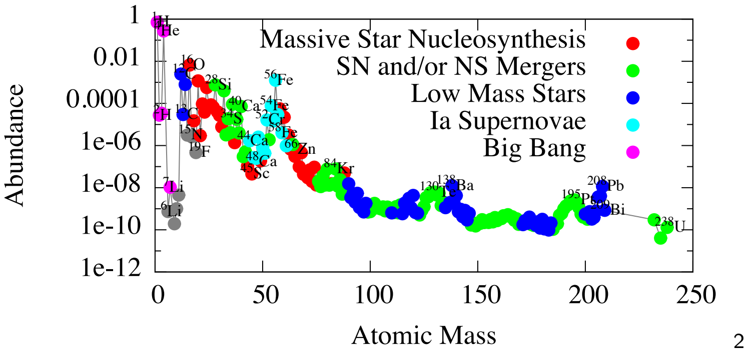

2 (Lodders, 2010; Woosley & Heger, 2002; Burbidge et al., 1957)

ODDC is modeled in stars using the Langer et al. (1983) prescription by deriving a diffusion coefficient, D.

MESA (Langer et al., 1983)

- Only mixes composition
- One free parameter, α

$$D = \frac{\alpha \kappa_T}{6} \frac{\frac{dT}{dz} - \left.\frac{\partial T}{\partial z}\right|_{\mathrm{ad}}}{\frac{\phi T}{\delta \mu}\frac{d\mu}{dz} + \left.\frac{\partial T}{\partial z}\right|_{\mathrm{ad}} - \frac{dT}{dz}} \tag{1}$$

$$\delta \equiv -\frac{\partial \ln \rho}{\partial \ln T}, \phi \equiv \frac{\partial \ln \rho}{\partial \ln \mu} \tag{2}$$

KEPLER (Woosley & Weaver, 1988)

- Only mixes composition
- One free parameter, F

$$D = \frac{F \kappa_T D_b}{F \kappa_T + D_b} \tag{3}$$

$$D_b \propto \left(\frac{dT}{dz} - \left.\frac{\partial T}{\partial z}\right|_{\mathrm{ad}}\right)^{\frac{1}{2}} \tag{4}$$

In particular, ODDC has strong relevance to stellar evolution because stellar cores are hot and heavy (Robertson & Faulkner, 1972).

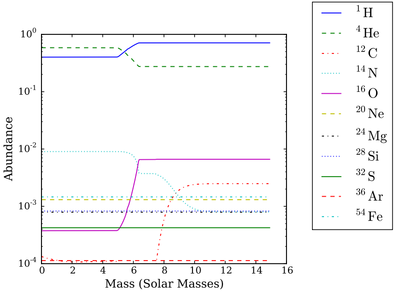

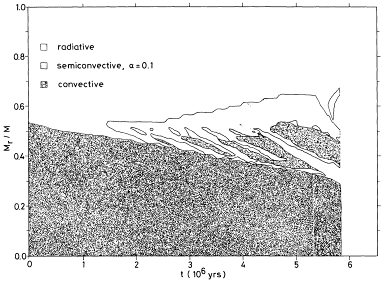

[3]

[3](Langer et al., 1985)

The later stages of massive stars are complex.

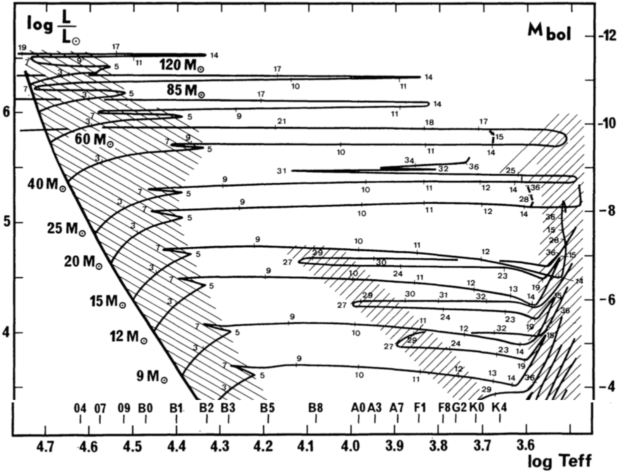

4

4 (Maeder & Meynet, 1988)

Since these late stages are dynamic, mixing processes (e.g. semi-convection) can drastically effect the final star structure and yields.

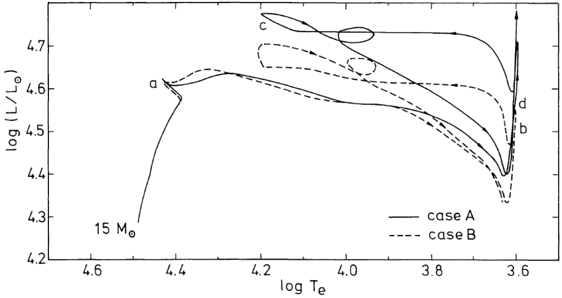

5

Figure: With semi-convection (solid), without (dashed)

[5] (Langer et al., 1985)

Small changes in the treatment of semi-convection can make the difference between stars becoming successful or failed supernovae by changing the final C/O cores.

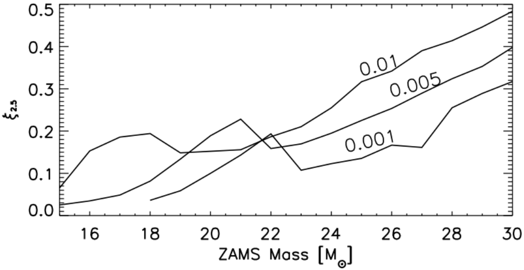

[6]

Figure: Likelihood of explosion, varying the semi-convection parameter from Woosley & Weaver (1988)

[6](Sukhbold & Woosley, 2014)

Overshooting convection is characterized by a convective region mixing into a nominally stable region.

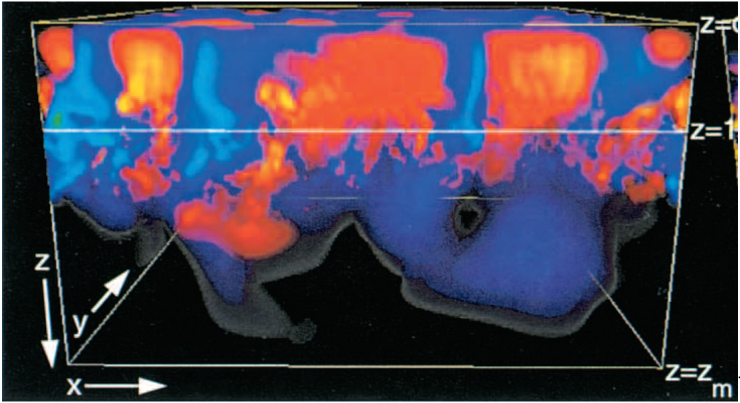

[7]

[7](Brummell et al., 2002)

This is distinct from penetrative convection, where the additional mixing extends the convection zone.

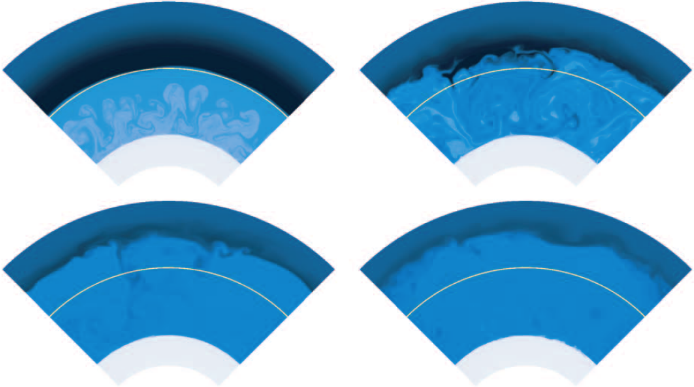

8

[8] (Meakin & Arnett, 2007)

Most numerical studies of overshooting convection investigate the effects of **stratification** at boundaries.

Some recent examples:

- Brummell et al. (2002)
- Meakin & Arnett (2007)
- Gilet et al. (2013)

Some convective boundaries are affected by varying **diffusion**, e.g. envelope convection and core helium burning.

Under the Boussinesq approximation, there are three possibilities for an overshooting region.

- A spatially-dependent thermal expansion coefficient
- A spatially-dependent heating term
- A spatially-dependent diffusion coefficient

Governing equations (Spiegel & Veronis, 1960)

Assuming the Boussinesq approximation and an adiabatic temperature gradient (such as appears during a formal derivation of the Boussinesq approximation for a gas) yields

$$\rho_0 \frac{D}{Dt}\mathbf{u} = -\nabla p + \rho_0 \alpha g T + \rho_0 \nu \nabla^2 \mathbf{u} \qquad (5)$$

$$\nabla \cdot \mathbf{u} = 0 \qquad (6)$$

$$\rho_0 \frac{D}{Dt} T - \rho_0 \left. \frac{d}{dz} T \right|_{\mathrm{ad}} = \rho_0 \nabla^2 \kappa_T(z) T + H(z) \qquad (7)$$

$$(8)$$

for the case with uniform diffusion but a z-dependent heating term.

Governing equations (Spiegel & Veronis, 1960)

or

$$\rho_0 \frac{D}{Dt}\mathbf{u} = -\nabla p + \rho_0 \alpha g T + \rho_0 \nu \nabla^2 \mathbf{u} \qquad (5)$$

$$\nabla \cdot \mathbf{u} = 0 \qquad (6)$$

$$\rho_0 \frac{D}{Dt} T - \rho_0 \left. \frac{d}{dz} T \right|_{\mathrm{ad}} = \rho_0 \nabla \cdot \left(\kappa_{T,0} + \kappa_T(z)\right) \nabla T \qquad (7)$$

$$(8)$$

for the case with nonuniform diffusion.

Governing equations (Spiegel & Veronis, 1960)

Subtracting a static background temperature and non-dimensionalizing yields

$$\frac{D}{Dt}\mathbf{u} = -\nabla p + \frac{\mathrm{Ra}_T}{\mathrm{Pr}} T + \nabla^2 \mathbf{u} \tag{5}$$

$$\nabla \cdot \mathbf{u} = 0 \tag{6}$$

$$\frac{D}{Dt} T + wf(z) = \nabla \cdot \left(\mathrm{Pr}^{-1} + \kappa_T(z)/\kappa_{T,0}\right)^{-1} \nabla T, \tag{7}$$

(8)

where $\kappa_T(z)$ is zero in the uniform diffusion case.

A simple solution to this is a spectral element code using Chebyshev polynomials in the vertical direction.

- Solves by Chebyshev collocation
  - Trivial to solve space-dependent diffusion
  - Fine resolution at element boundaries
  - Coarse resolution at element centers

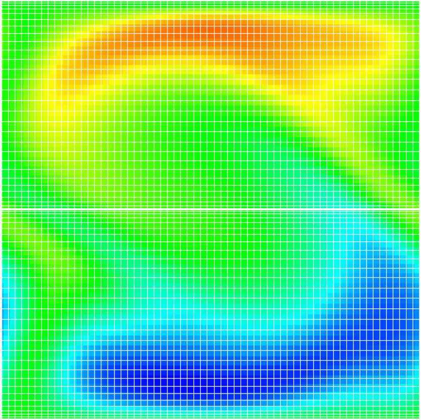

We've run simulations in 2D and 3D with PADDI, and find similar results—except in particular cases with strong shear.

$\mathrm{Pr} = 0.03$
$\tau = 0.3$
$R_0^{-1} = 1.1, 1.2$

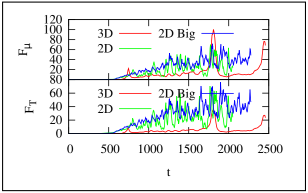

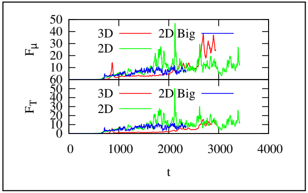

$\mathrm{Pr} = 0.01$
$\tau = 0.01$
$R_0^{-1} = 1.5, 2$

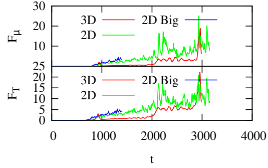

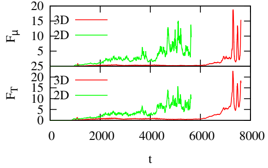

At early stages, the simulations have similar behavior; however, at late stages, large shear dominates the 2D runs.

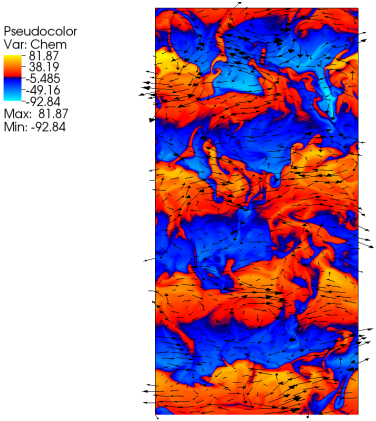

Figure: $\mathrm{Pr} = 0.3$, $\tau = 0.3$, $R_0^{-1} = 1.15$

At early stages, the simulations have similar behavior; however, at late stages, large shear dominates the 2D runs.

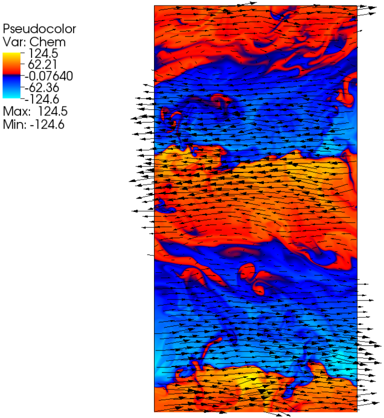

Figure: $\mathrm{Pr} = 0.3$, $\tau = 0.3$, $R_0^{-1} = 1.15$

Fortunately, this problem appears absent in the low viscosity and compositional diffusivity runs at low R_0^{-1}.

$\mathrm{Pr} = 0.03$
$\tau = 0.3$
$R_0^{-1} = 1.1, 1.2$

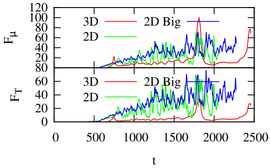

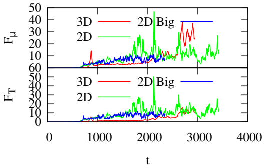

$\mathrm{Pr} = 0.01$
$\tau = 0.01$
$R_0^{-1} = 1.5, 2$

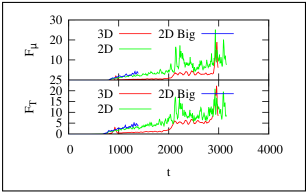

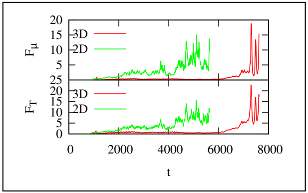

These simulations show no sign of the strong horizontal shear apparent in the simulations at higher viscosity.

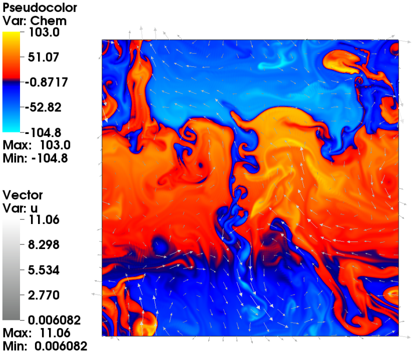

Figure: $\mathrm{Pr} = 0.03$, $\tau = 0.03$, $R_0^{-1} = 1.5$

Boundary conditions

- Fixed outer vertical boundaries
- Periodic horizontal boundaries
- Cross-element boundaries must be continuous and smooth

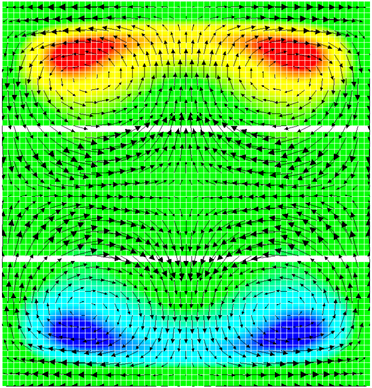

The code currently constrains the velocity using a predictor-corrector method according to the incompressible velocity constraint (Chorin, 1997).

$$\nabla \cdot \mathbf{u}^{\mathrm{new}} = 0 \tag{9}$$

Update the velocity according to the momentum equation, ignoring the pressure term.

$$\rho_0 \frac{D}{Dt} \mathbf{u}^{\mathrm{mid}} = \left(-\alpha T + \beta \mu\right) \rho_0 \mathbf{g} + \nu \rho_0 \nabla^2 \mathbf{u}^{\mathrm{mid}} \tag{10}$$

$$\frac{\mathbf{u}^{\mathrm{new}} - \mathbf{u}^{\mathrm{mid}}}{\Delta t} = - \frac{\nabla p}{\rho_0} \tag{11}$$

$$\frac{-\nabla \cdot \mathbf{u}^{\mathrm{mid}}}{\Delta t} = - \nabla \cdot \frac{\nabla p}{\rho_0} \tag{12}$$

The code is pseudo-spectral, calculating the non-linear terms in Cartesian space and implicit terms in spectral space.

- Fourier series in the horizontal to enforce periodicity
- Chebyshev polynomials in the vertical for fine boundary resolution

$$F(x,z) = \sum_{j=-N_x/2}^{N_x/2} \sum_{k=0}^{N_z} f_{i,j} e^{\frac{2\pi ij(x-x_0)}{L_x}} T_k\left(\frac{z-z_0}{L_z/2}\right) \tag{13}$$

The code solves the diffusion implicitly by alternating directions, solving by collocation in the vertical and by spectral method in the horizontal.

$$\sum_k \left(T_k \left(\frac{z_l - z_0}{L_z/2} \right) - \kappa \left(z_l \right) \frac{\Delta t}{L_z^2/4} T_k'' \left(\frac{z_l - z_0}{L_z/2} \right) \right) f_{j,k}^{\mathrm{new}} = F_j^{\mathrm{old}} \left(z_l \right) + \Delta t RHS_j \left(z_l \right) \quad (14)$$

We can solve equations with z-dependent coefficients implicitly

$$\left(1 - \kappa \left(z_l \right) \Delta t \left(\frac{2\pi i j}{L_x} \right)^2 \right) F_j^{\mathrm{new}} \left(z_l \right) = F_j^{\mathrm{old}} \left(z_l \right) + \Delta t RHS_j \left(z_l \right) \quad (15)$$

The collocation method matches the boundaries of the elements with spectral accuracy; the matrix can be solved as follows (Beaume, private communication).

$$\begin{pmatrix} A_{0,0} & A_{1,0} & 0 & 0 & \dots & 0 & 0 \\ A_{0,1} & A_{1,1} & A_{2,1} & 0 & \dots & 0 & 0 \\ 0 & A_{1,2} & A_{2,2} & A_{3,2} & \dots & 0 & 0 \\ 0 & 0 & A_{2,3} & A_{3,3} & \dots & 0 & 0 \\ \vdots & \vdots & \vdots & \vdots & \ddots & A_{N-2,N-3} & 0 \\ 0 & 0 & 0 & 0 & A_{N-3,N-2} & A_{N-2,N-2} & A_{N-1,N-2} \\ 0 & 0 & 0 & 0 & 0 & A_{N-2,N-1} & A_{N-1,N-1} \end{pmatrix} \begin{pmatrix} X_0 \\ X_1 \\ X_2 \\ X_3 \\ \vdots \\ X_{N-2} \\ X_{N-1} \end{pmatrix} = \begin{pmatrix} B_0 \\ B_1 \\ B_2 \\ B_3 \\ \vdots \\ B_{N-2} \\ B_{N-1} \end{pmatrix}$$

The collocation method matches the boundaries of the elements with spectral accuracy; the matrix can be solved as follows (Beaume, private communication).

$$
\left(\begin{array}{ccccc|cccc}
A_{0,0} & 0 & \dots & \dots & 0 & A_{1,0} & 0 & \dots & 0 \\
0 & A_{2,2} & \dots & \dots & 0 & A_{1,2} & A_{3,2} & \dots & 0 \\
\vdots & \vdots & \ddots & \dots & \vdots & \vdots & \ddots & \ddots & \vdots \\
0 & 0 & \dots & \ddots & 0 & 0 & 0 & \ddots & A_{N-2,N-3} \\
0 & 0 & \dots & \dots & A_{N-1,N-1} & 0 & 0 & \dots & A_{N-2,N-1} \\
\hline
A_{0,1} & A_{2,1} & \dots & 0 & 0 & A_{1,1} & 0 & \dots & 0 \\
0 & A_{2,3} & \ddots & 0 & 0 & 0 & A_{3,3} & \dots & 0 \\
\vdots & \vdots & \ddots & \ddots & \vdots & \vdots & \vdots & \ddots & \vdots \\
0 & 0 & \dots & A_{N-3,N-2} & A_{N-1,N-2} & 0 & 0 & \dots & A_{N-2,N-2}
\end{array}\right)
$$

The collocation method matches the boundaries of the elements with spectral accuracy; the matrix can be solved as follows (Beaume, private communication).

$$\begin{pmatrix} A_{TL} & A_{TR} \\ A_{BL} & A_{BR} \end{pmatrix} \begin{pmatrix} X_L \\ X_R \end{pmatrix} = \begin{pmatrix} B_T \\ B_B \end{pmatrix} \tag{16}$$

$$A_{TL} X_L + A_{TR} X_R = B_T \tag{17}$$

$$A_{BL} X_L + A_{BL} A_{TL}^{-1} A_{TR} X_R = A_{BL} A_{TL}^{-1} B_T \tag{18}$$

$$\begin{pmatrix} A_{TL} & 0 \\ 0 & A_{BR} - A_{BL} A_{TL}^{-1} A_{TR} \end{pmatrix} \begin{pmatrix} X_L + A_{TR} X_R \\ X_R \end{pmatrix} = \tag{19}$$

$$\begin{pmatrix} B_T \\ B_B - A_{BL} A_{TL}^{-1} B_T \end{pmatrix} \tag{20}$$

The extents of these elements are dynamic, and can be rezoned using simulated annealing.

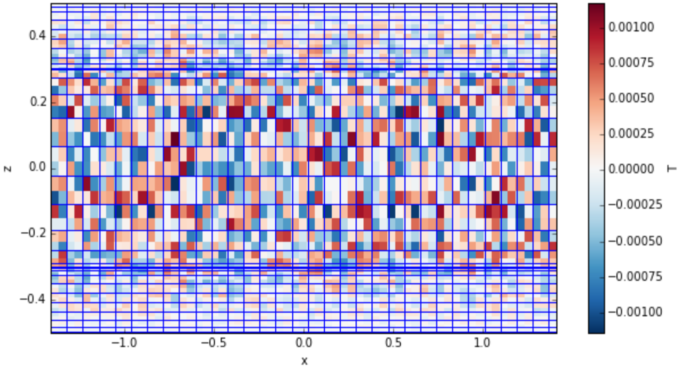

To verify the code, we ran the standard Rayleigh Bénard Convection problem and compared to Moore & Weiss (1973).

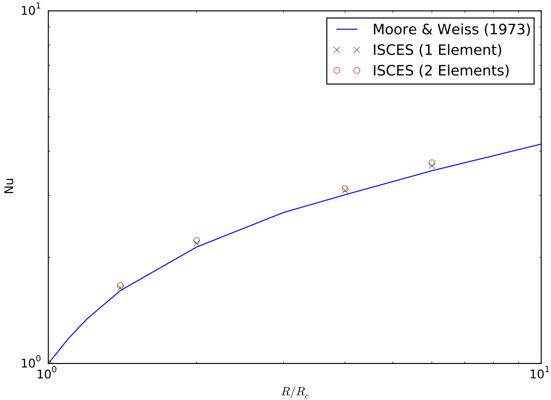

We can also compare to the results of the same equations with the same parameters as PADDI.

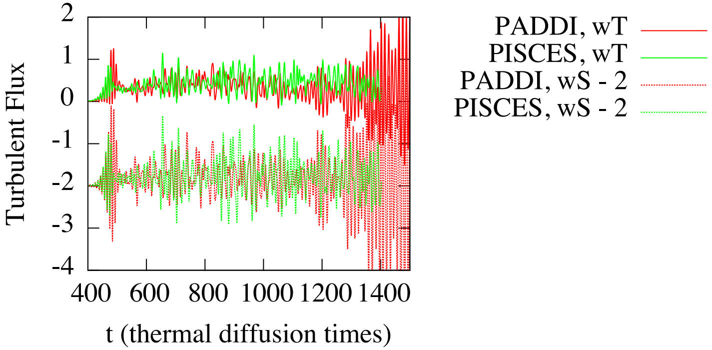

Figure: The late time behavior is dominated by the boundary conditions, which differ between the codes

We are investigating the differences between heating and variable diffusion.

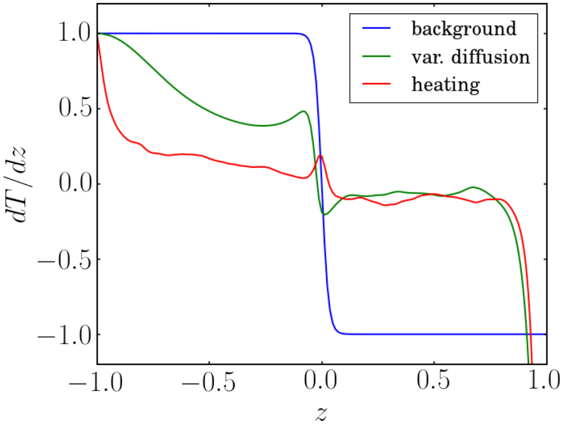

Mixing in Stars

PISCES

Future

Brummell, N. H., Clune, T. L., & Toomre, J. 2002, The Astrophysical Journal, 570, 825

Burbidge, E., Burbidge, G., Fowler, W., & Hoyle, F. 1957, Reviews of Modern Physics, 29, 547

Chorin, A. 1997, Journal of computational physics, 135, 118

Garaud, P. 2014, eprint arXiv:1401.0928

Gilet, C., Almgren, A. S., Bell, J. B., Nonaka, A., Woosley, S. E., & Zingale, M. 2013, The Astrophysical Journal, 772, 1

Langer, N., El Eid, M. F., & Fricke, K. J. 1985, Astronomy & Astrophysics, 145, 179

Langer, N., Sugimoto, D., & Fricke, K. J. 1983, Astronomy & Astrophysics, 126, 207

Lodders, K. 2010, in Principles and Perspectives in Cosmochemistry, ed. A. Goswami & B. E. Reddy, Astrophysics and Space Science Proceedings (Berlin, Heidelberg: Springer Berlin Heidelberg)

Maeder, A. & Meynet, G. 1988, Astronomy and Astrophysics, Suppl. Ser., Vol. 76, p. 411-425 (1988)

Meakin, C. A. & Arnett, D. 2007, The Astrophysical Journal, 667, 448

Moore, D. R. & Weiss, N. O. 1973, Journal of Fluid Mechanics, 58, 289

Robertson, J. W. & Faulkner, D. J. 1972, The Astrophysical Journal, 171, 309

Spiegel, E. & Veronis, G. 1960, Astrophysical Journal, 131, 442

Sukhbold, T. & Woosley, S. E. 2014, The Astrophysical Journal, 783, 10

Woosley, S. E. & Heger, A. 2002, Reviews of Modern Physics, 74, 1015

Woosley, S. E. & Weaver, T. A. 1988, Physics Reports, 163, 79